The Geometry of the Obscurer in a Dusty Hyperluminous Quasar

Duncan Farrah, Mislav Balokovic, Daniel Stern, Kathryn Harris, Michelle Kunimoto, Dominic Walton, et al

Farrah et al, ApJ, accepted, astroph 1606.05649, *farrah@vt.edu*

AGN unification

explains the observed plethora of AGN types based on there existing an axisymmetric obscurer in AGN, where the line of sight to, and structure of, the obscurer gives rise to the observed properties of that AGN. Testing this model is however a profound challenge, as observations at different wavelengths give incomplete information on different parts of the obscuring structure. Moreover, since the AGN obscurer spans scales of less than a kiloparsec, it is difficult to spatially resolve, especially outside of the local Universe

In this poster

we study the AGN obscurer in a luminous quasar at z=0.44. We combine data from the infrared and X-ray to constrain the geometry, and optical data to assign an absolute scale. This approach offers the possibility to constrain obscurer geometries across a wide range in redshift.

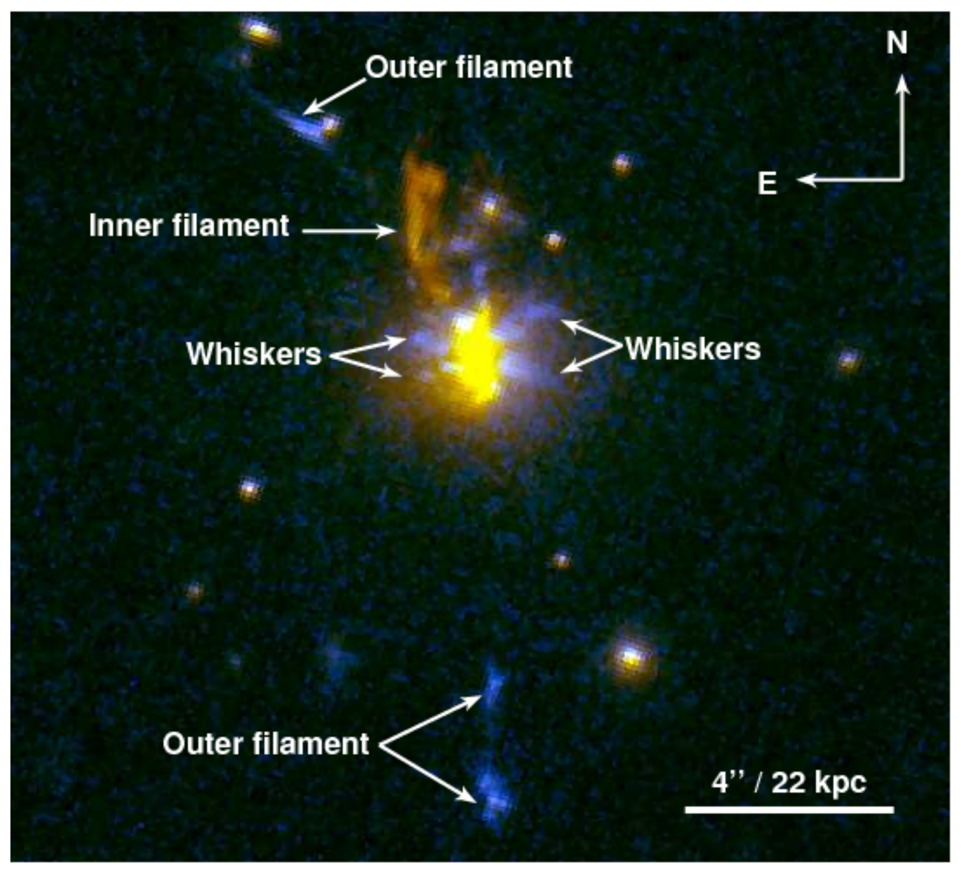

Our Target

is IRAS 09104+4109 (hereafter P09104). It is extremely IR-luminous but with a small mass of H_2 and only 10^7 M_{sun} of warm dust. It has a Sy2 spectrum, but with a broad Hb line in polarized light. Optical imaging from O'Sullivan et al 2012 reveals a disturbed system with several bright `knots', multiple companions, and extended filaments.

In the infrared

we assembled data from several sources. From *Spitzer* we obtained photometry from IRAC at 3.6 and 4.5um, and a 6-34um spectrum from the IRS. From *Herschel*, we obtained photometry at 70, 100, and 160um from PACS, and at 250, 350, and 500um from SPIRE. Finally, we obtained an 850um SCUBA measurement from Deane et al 2001.

We fitted the infrared data with two grids of radiative transfer models; one for AGN and one for starbursts. The AGN models assume a smooth tapered disk geometry whose height increases linearly with distance from the AGN until it reaches a constant value. The dust distribution includes multiple species, and assumes the density distribution scales as r^{-1}. The AGN model parameters are: inner half-opening angle of the torus, viewing angle (both measured from pole-on), ratio of inner to outer disc radius, and ratio of height to outer radius. The resulting best-fit IR SED is:

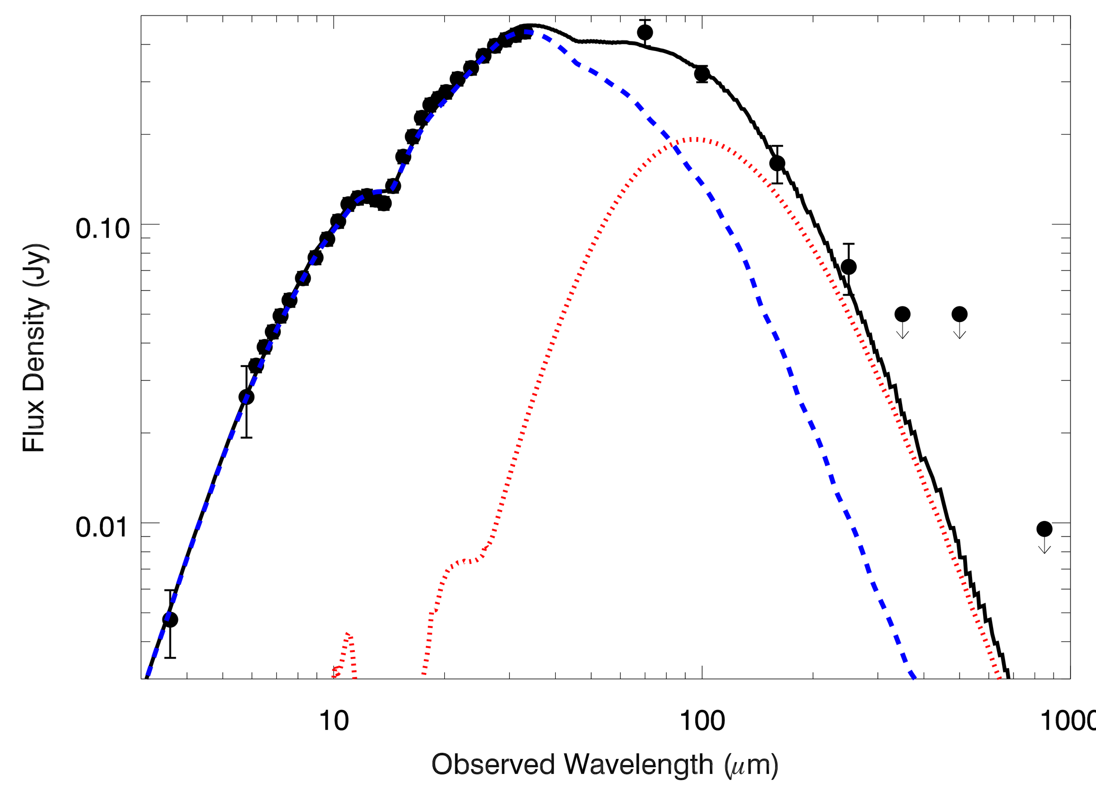

The black line is the combined model, the blue line is the AGN, and the red line is the starburst. The total IR (rest-frame 1-1000um) luminosity is 6.76×10^{46} erg s^{-1}, with a contribution from the AGN of 5.94×10^{46} erg s^{-1}. The viewing angle to the torus is ~35 degrees. The half opening angle of the torus is indistinguishable from the viewing angle. The inner to outer radius ratio of the torus is ~0.016, while the ratio of the torus height to the outer radius is ~0.16. The starburst has a star formation rate of 110M_{sun} yr^{-1}, and an age of <50Myr.

In the X-ray

we observed P09104 with *NuSTAR* for 15.3ks. The observations were coordinated with *Swift*. We complemented these data with archival data from *Suzaku* and *Chandra*, both taken within three years of the *NuSTAR* data.

To model the soft X-ray data we used two Mekal plasmas. To model the hard X-ray data we use two models. First, a model consisting of transmitted (T) and reflected (R) components. The T component is an absorbed power law. The R component has a Gaussian line at 6.4 keV. Second, two observationally motivated models; MYtorus and BNtorus. Both MYtorus and BNtorus assume a smooth toroidal obscurer geometry. The best-fit T+R and torus models are:

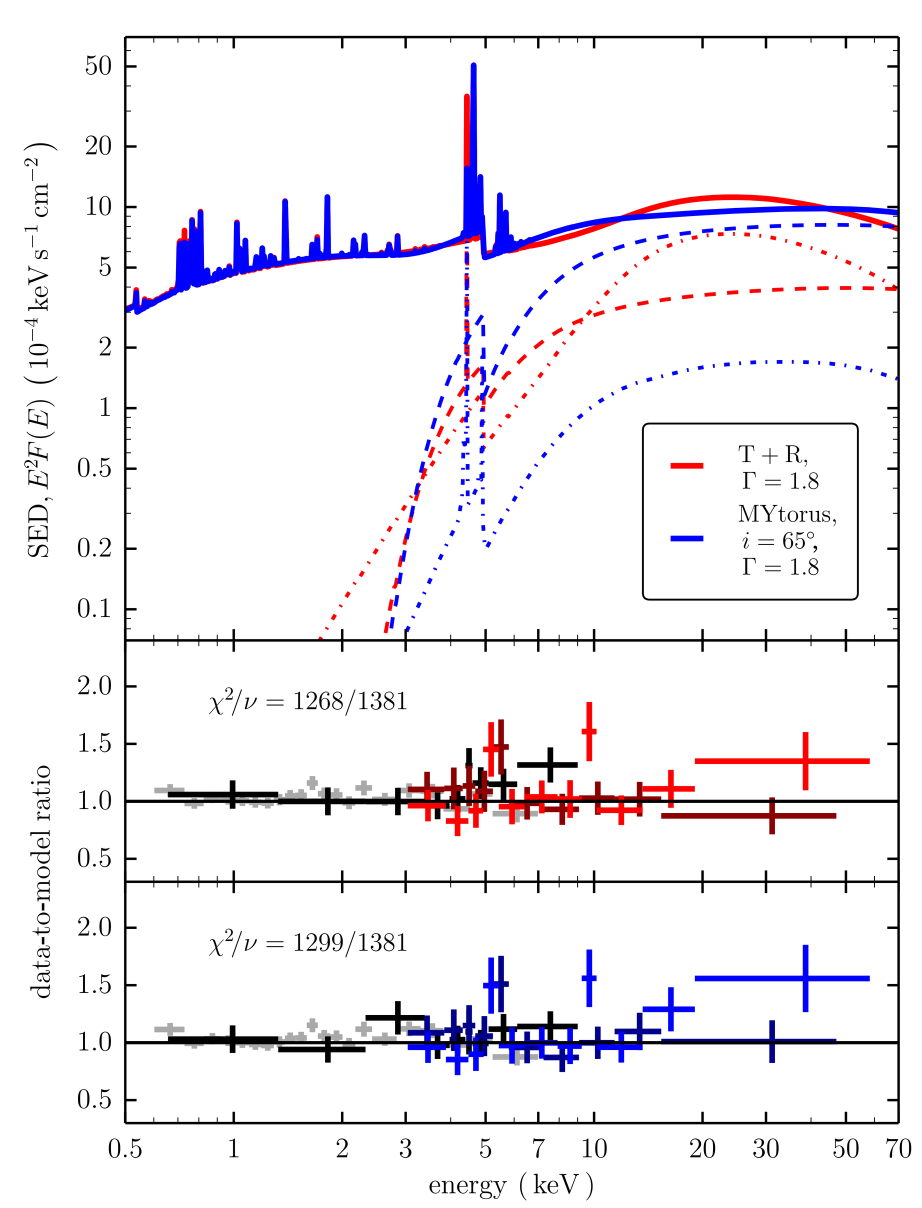

The T+R model fit is shown by the red lines, while the blue lines show a MYtorus model. Solid lines are for the total spectrum (AGN and diffuse emission), dashed lines are for the transmission components, and dot-dashed lines are for the reflection components. Plasma components making up the diffuse emission are not plotted in order to avoid confusion; any flux not contributed by the AGN components is due to plasma emission. The lower panels show the data-to-model ratio for each of the two models. Colored lines are for *NuSTAR*, grey is for *Suzaku*, and black is for *Chandra*. For the T+R model, the results depend significantly on the value of the photon index, as shown below:

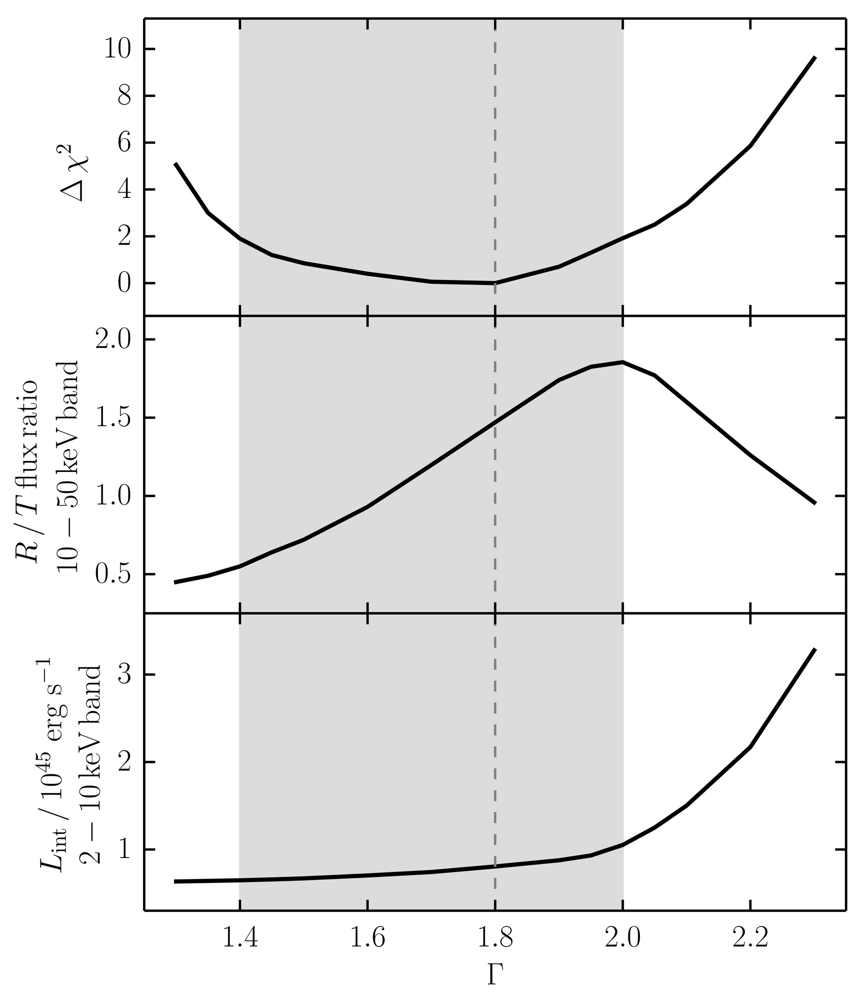

Overall, the X-ray data are consistent with Γ~1.8 and N_H ~ 5×10^{23} cm^{-2}. The soft X-ray data alone drive the fit toward Γ<1.5 and a T dominated solution, but the addition of *NuSTAR* data results in a solution where T and R components contribute at comparable levels, and rules out an R dominated scenario in which line-of-sight obscuration and intrinsic luminosity would be much higher.

We see consistency

in the constraints on the AGN obscurer geometry from the X-ray and infrared data. Fixing the half-opening angle to 39 degrees in BNtorus gives a best-fit viewing angle of 48 degrees. This combination of viewing and half-opening angles coincides with a broad minimum in χ^2 for all the BNtorus model fits, and is within 1 sigma of the IR-based half-opening and viewing angles. The MYtorus constraints are similar. The X-ray and infrared torus models are thus both consistent with scenarios where the line of sight viewing angle is close to the half-opening angle. The data do not favor extreme geometries, such as edge-on viewing angle, or tori that are disk-like or sphere-like. This "skimming" of the edge of the torus by the line-of-sight viewing angle suggests that, had P09104 been viewed at a viewing angle smaller by only a few degrees, it would have been classified as a broad-line object in direct light.

Setting the scale:

We obtained an optical spectrum of P09104 at Palomar:

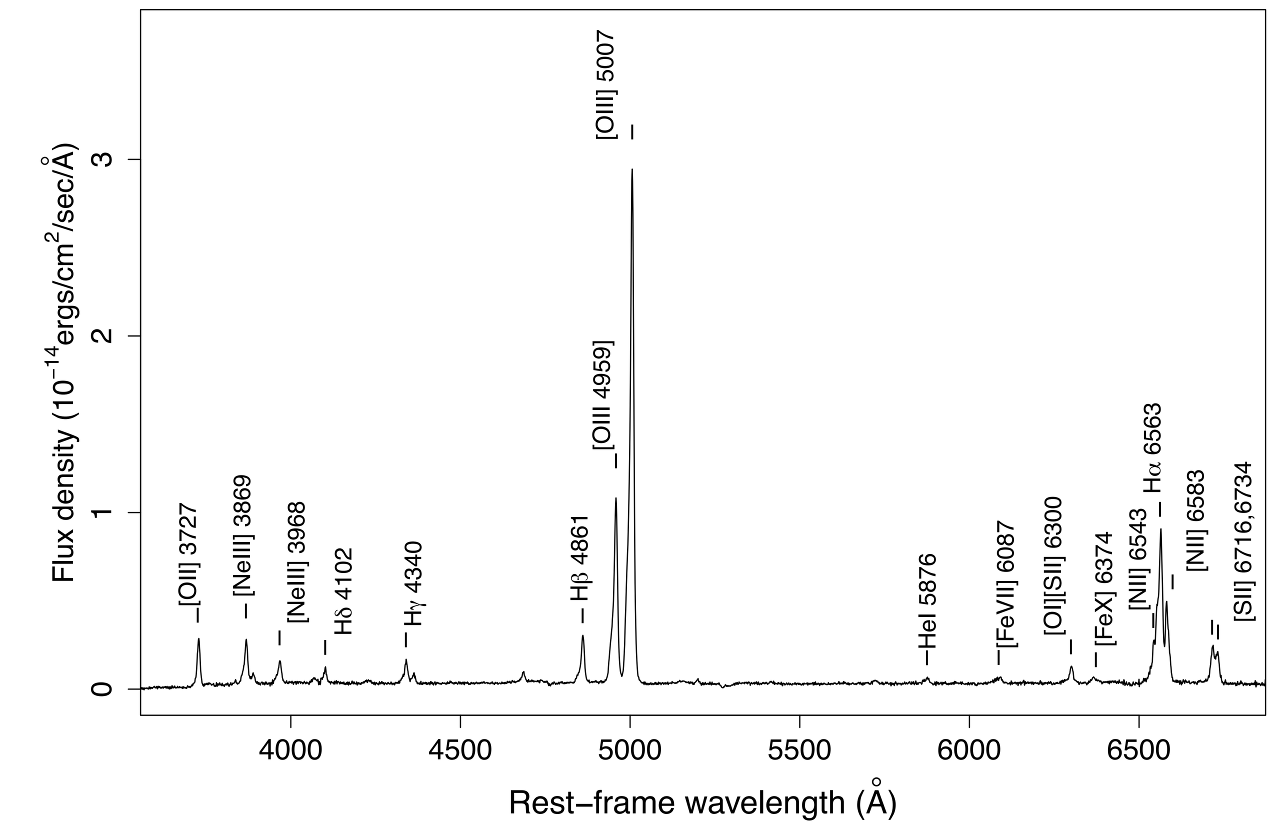

The high excitation iron lines in this spectrum have several possible origins, but the most plausible is a Coronal Line Region (CLR) intermediate in distance between the BLR and NLR. The detection of [Fe X]6375 but not [Fe XIV]5303 implies a line of sight to a distance from the central ionizing source of 0.2-20pc

Putting everything together:

The X-ray and infrared data together give a consistent geometry of the obscurer in P09104 The detection of high excitation iron lines in the optical provides further constraints - their detection is also consistent with a line of sight that skims the torus - the CLR is visible in direct light but the BLR can only be seen in scattered light. Taking the distance constraints from the detection of [Fe X] but not [Fe XIV] then places the bulk of the IR-emitting torus to within a vertical height of 20pc of the nucleus. The X-ray obscurer is thus plausibly within this distance, also. This then places the outer `edge' of the IR-emitting torus within 125pc of the nucleus and the inner edge within 2pc. A sketch of the obscurer structure consistent with the combined dataset is:

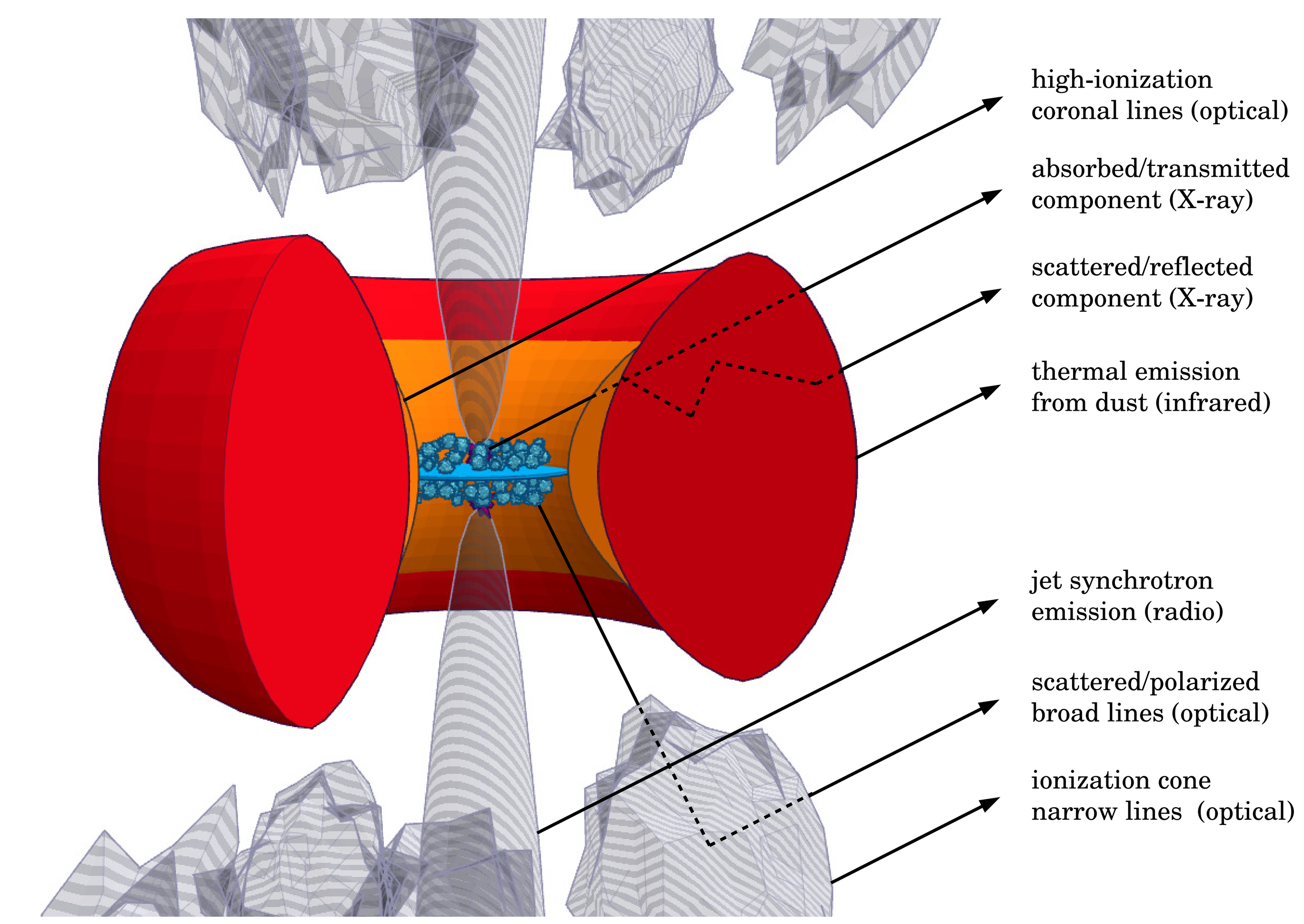

The observer is in the direction of the arrows. The torus is shown in red. IR emission is due to dust in the torus, while the coronal lines in the optical spectrum come from the torus inner side (orange). X-rays pass through the torus; we distinguish contributions from the absorbed line-of-sight component (transmission; T) and from the component due to scattering (reflection; R). The accretion disk and the BLR are shown in blue, and the jet and NLR are shown in grey. The BLR is shielded from direct view by the vertical extent of the torus, but scattering in the ionization cones makes broad lines observable in polarized light. The ionization cones also emit narrow forbidden lines, and the jet is observable at radio wavelengths.